DOI: https://doi.org/10.24425/amm.2025.154480

VU NGOC HAI<sup>©</sup><sup>1\*</sup>, S. LEE<sup>1</sup>, T. TSUCHIYA<sup>1</sup>, T. KATSUMI<sup>2</sup>, K. KITA<sup>2</sup>, K. MATSUDA<sup>1\*</sup>

## EFFECT OF PRE-AGING TEMPERATURE ON HARDENING BEHAVIOR AND PRECIPITATION RESPONSE OF DEFORMED Al-1.0%Cu-0.96%Mg-0.36%Si (wt.%) ALLOY

In the Al-1.0%Cu-0.96%Mg-0.36%Si alloy, it has been found that pre-aging before deformation is very important in controlling the precipitation characteristics of the alloy during the subsequent artificial aging process. Pre-aging temperature significantly affects these properties by causing changes in the main precipitates, while the alloy composition influences the overall material behavior. For the detailed pre-aging temperature investigations, the mechanical tests, the dislocation density evolution, and the microstructure changes were examined by transmission electron microscopy, X-ray diffraction analysis and Vickers hardness measurement. The conclusions provide that the hardness and dislocation density increase as the pre-aging temperature go up. In this work, the deformation with the precipitation formation in the pre-aging period may enable such changes in the predominate precipitation in artificial aging.

Keywords: Aluminum alloys; pre-aging; precipitation; dislocation density; hardness

#### 1. Introduction

The growing emphasis on environmental protection and energy efficiency has increased demand for weight reduction in automobiles [1]. Various Al-Cu-Mg-Si alloys have been developed based on the Al alloys. Such alloys can be made stronger by precipitation hardening of several metastable phases achieved by artificial aging. In engineering practice, doing an artificial aging process right after the solution heat treatment is quite challenging [2]. As a result, deferring the initiation of pre-aging by room temperature storage, refrigeration, or even pre-aging at higher temperature before artificial aging is needed. In industrial manufacturing, there is typically a period of room temperature storage of the material before conducting the artificial aging, during which the strength of the alloy is increasing [3]. Natural aging is credited mainly to the concentration of solute elements in the matrix at room temperature over time. Cao et al. [4] found that the hardness of the T6 Al-Mg-Si-Cu alloys rapidly decreased with increasing room temperature storage times of 2 to 3 hours. Pre-aging is unlikely to change the size and distribution and will be more hardenable during aging [5]. Pre-aging affects various thermal aging responses in alloys. Even though there is a body of literature focusing on the influence of pre-aging at low temperature on age-hardening, multicategory data interpretation regarding both natural aging and pre-aging effects is rare [6]. In this paper, our results are focused on the analysis of the influence of pre-aging at 0°C and 35°C on the mechanical properties and microstructural changes of Al-1.0%Cu-0.96%Mg-0.36%Si alloy using hardness tests and transmission electron microscopy. In addition, dislocation density is assessed because this parameter is essential in distinguishing the differences between pre-aging at 0°C and 35°C.

### 2. Experimental procedure

The alloy composition used in this study was Al-1.00%Cu-0.96%Mg-0.36%Si (wt.%). The samples were solution treated at 505°C for 3 hours and then quenched to room temperature using ice water. Pre-aging at 0°C was performed using a simulated refrigerator while pre-aging at 35°C was performed when the samples quenched were immersed in an oil bath. All the samples were subjected to a one-week holding time before a cold deformation of 30% in reduction was applied, and they were subjected to an artificial aging temperature of 160°C. Various processing conditions for as-quenched samples are shown in TABLE 1.

<sup>\*</sup> Corresponding authors: matsuda@sus.u-toyama.ac.jp, vungochaibk61@gmail.com



UNIVERSITY OF TOYAMA GRADUATE SCHOOL OF SCIENCE AND ENGINEERING FOR RESEARCH, JAPAN

<sup>&</sup>lt;sup>2</sup> MACHINERY AND ENGINEERING GROUP, YKK CORPORATION, JAPAN

The Vickers hardness of the samples  $(10 \times 10 \times 2 \text{ mm}^3)$  was measured **at room-temperature** Mitutoyo HM-101 hardness tester. A force of 0.98 N was applied for fifteen seconds. The TEM samples were thinned by mechanical polishing to a thickness of 0.08 mm and electro-polishing with the twin-jet method. The electrolyte used had a 1:3 ratio of HNO3 to methanol, which was kept at a low temperature ( $-20^{\circ}$ C to  $-30^{\circ}$ C) during polishing. A TEM TOPCON RM-002B microscope was utilized for this type of observation. Also, the dislocation density was calculated by X-ray diffraction analysis with Rigaku Ultima IV machine.

TABLE 1 Various processing conditions for as-quenched samples

Samples	Treatment
H01	SHT + PA 0°C + deformation 30% +
	artificial aging 160°C
H02	SHT + PA 35°C + deformation 30% +
	artificial aging 160°C

#### 3. Results and discussions

### 3.1. Effect of pre-aging on the age-hardening behavior of the alloy

In order to investigate the effect of pre-aging on the agehardening behavior of the alloy, changes in Vickers hardness (HV) with prolonged aging time in samples H01 and H02, aged for 2 to 10,000 minutes at 160°C as shown in Fig. 1. The hardness curve indicated that the hardness of H02 was higher than H01. After one week of pre-aging, H01 and H02 hardness values reached 45 HV and 75 HV, respectively. It was reported that the hardness of all the samples increased after deformation 30%, which was found to be more pronounced with the higher pre-aging **temperature**. In this regard, the pre-aging measures not only enhance the strength of the alloy but also reduce the total aging time [5]. Upon water quenching of the high-temperature

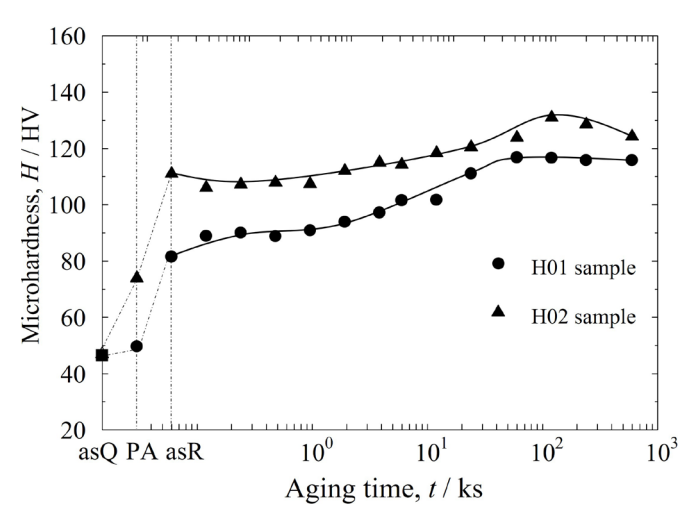


Fig. 1. Age hardening curves of Al-1.00%Cu-0.98%Mg-0.36%Si alloy pre-aged at 0, 35°C, deformation 30% and then aged at 160°C for various times

solution treated condition, most of the atoms stay in the matrix and are in the form of supersaturated solid solution. The diffusion of Cu, Mg, and Si atoms through the Al matrix follows temperature and vacancy concentration as major controlling factors [7]. Pre-aged samples were held at 0°C for one week, as basically all pre-aged atoms stayed within the matrix thus there was very little pre-aging effects on the hardness. However, pre-aging at 35°C could confirm that the cluster formed. The clusters take up a significant part of the vacancies created by the quenching, hence improving hardness after pre-aging [8]. These clusters also provide sites for the growth of precipitates during the early stages of artificial aging. The creation of nano-sized clusters before deformation and artificial aging enhancement to this effect [9].

#### 3.2. Dislocation density from XRD analyze

The influence of the pre-aging on the mechanical properties was examined by measuring dislocation density using X-ray diffraction analysis. X-ray diffraction offers valuable information regarding the crystal structure of a material, therefore defining the dislocation density, which mainly dictates the mechanical properties. High-resolution  $2\theta$  scans of the (111), (200), (220), and (311)Al diffraction peaks were carried out to assess the effect of raising the pre-aged temperature in the case of deformation and artificial aging, as shown in Fig. 2. Several methods were employed to verify the dislocation density increase. The graphs of  $(2\sin\theta/\lambda)$  and  $(2\beta\cos\theta/\lambda)$ , which is referred to as the Williamson-Hall (WH) method as shown Fig. 3(a,b). The width of the XRD peak, designated as  $\beta$ , is shown to depend upon the strain through the WH equation [19]:

$$\beta \frac{\cos \theta}{\lambda} = \alpha + 2\varepsilon \frac{\sin \theta}{\lambda} \tag{1}$$

$$\alpha = \frac{0.9}{D} \tag{2}$$

where,  $\theta$  is the diffraction angle,  $\lambda$  is the X-ray wavelength,  $\varepsilon$  is the strain, and D is the size of average particle. The  $\beta$  parameter is obtained on  $2\theta$ . The density of dislocation states  $\rho$  can therefore be defined with:

$$\rho = 14.4 \frac{\varepsilon^2}{b^2} \tag{3}$$

here, b is a parameter that characterizes the size of Burger's vector.

In many cases, a pronounced anisotropy in the broadening of lines was observed, the  $(\beta \cos \theta/\lambda)$  cannot be a monotonous function of  $\sin \theta$ . The dislocations in the deformed crystals are responsible for enhancing peak-width and peak-width anisotropy [20,21]. To address this issue, Ungar at el. [22] modified the WH equation exploiting the kinematical diffraction theory of distorted crystal. Dislocation density values were subsequently calculated using the Modified Williamson-Hall (MWH) plots

as shown in Fig. 3(c, d), to fit  $\Delta K$  as a linear function, using the relationship [23]:

$$\left(\Delta K\right)^2 = \left(\frac{0.9}{D}\right)^2 + \frac{\pi M^2 b^2}{2} \rho K^2 \overline{C} \tag{4}$$

Where K is the equivalent diffraction angle of each diffraction peak in reciprocal space  $(2\sin\theta/\lambda)$ ,  $\bar{C}$  is the contrast coefficient of the dislocation, b is the Burger vector, and  $\Delta K$  is the experimentally observed full width at half maximum (FWHM) of each diffraction peak, it is unknown but expected to be between 1 and 2 in this context [24].

The dislocation density ( $\rho$ ) results obtained from the fitted lines as shown in Fig. 3. For the sample pre-aging at 0°C and 35°C, the dislocation density determined to be  $0.9 \times 10^{15} \text{m}^{-2}$  and  $2.9 \times 10^{15} \text{m}^{-2}$ , respectively. The data show that higher pre-aging temperature before deformation increase the dislocation density. This result highlights the significant impact the pre-aging temperature on the hardening behavior and precipitation response of the alloy. Pre-aging at 35°C forms fine precipitates in the alloy before deformation and artificial aging [8]. These precipitates help to constrain the motion of dislocations in later deformation steps. The choice of a base-appropriate pre-aging temperature is critical since it helps in determining the size, distribution, and density of these

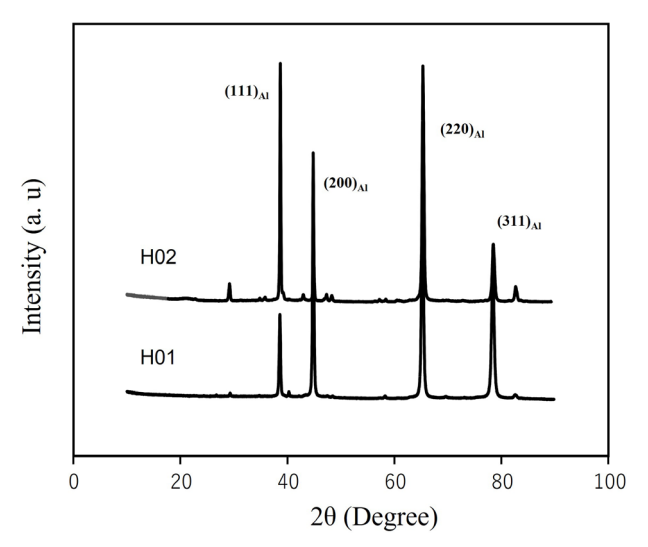


Fig. 2. XRD pattern of samples: H01, and H02 after deformation

precipitates [7]. With an increase in pre-aging temperature, the alloying elements in the matrix will tend to diffuse in greater proportions, and that is one factor leading to changes in the nucleation and growth of precipitates [5]. This can result in a higher dislocation density after deformation, as dislocation encounters more obstacles in the form of larger and more widely distributed precipitation [25].

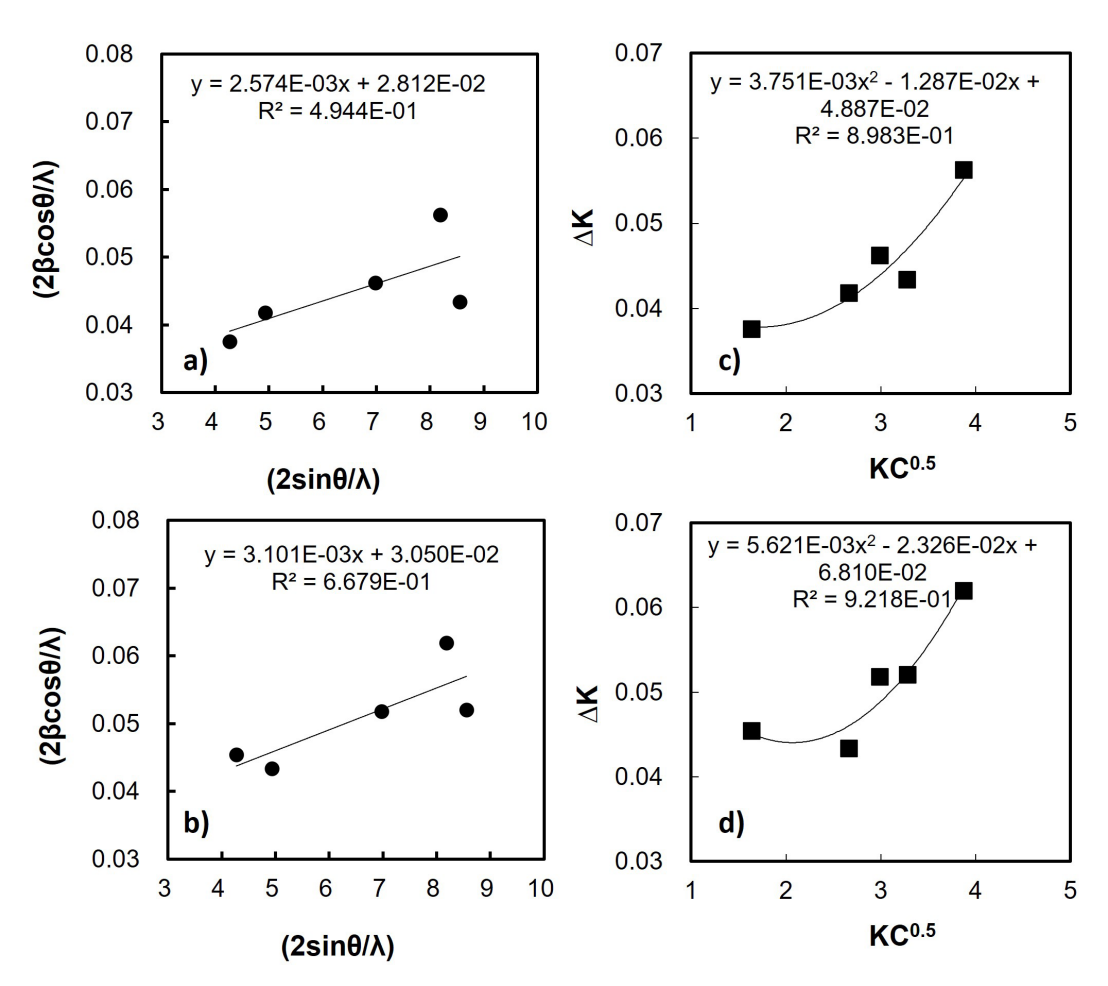


Fig. 3. Plots of  $(2\sin\theta/\lambda)$  and  $(2\beta\cos\theta/\lambda)$  from Williamson-Hall (WH) method and Plots of Modified Williamson-Hall method (MWH); (a, c) H01 sample; (b, d) H02 sample

# 3.3. Effect of pre-aging the precipitation response on artificial aging

Precipitation response in the H01 sample which is pre-aged at 0°C, followed by 30% cold deformation and artificial aging at 160°C under peak aging condition as shown in Fig. 4. In this condition, precipitates were observed to be small rod-shaped and needle shape  $\beta''$  precipitates found in the <010> direction within the Al matrix as in Fig. 4(e) and Fig. 4(f), respectively. Additionally, in Fig. 4(d), the distribution of precipitates in sample H01 contains three different types at dislocation. Region (1) indicates the disordered matrix in which phase C is formed. Phase C was first reported by Marioara et al. [10]. Region (2), those elongated precipitates are formed relatively parallel to the  $<1\overline{1}0>$  and termed as from "phase E." E. Thronsen et al. [11] discovered E phase contested during the aging process of pre-deformed Al-1.3Cu-1.0Mg-0.4Si (wt.%) alloy. Finally, region (3) displays a lath-like precipitate of the S' phase, known to occur usually at dislocations [12].

Precipitation response in the H02 sample which is preaged at 35°C, followed by 30% cold deformation and artificial aging at 160°C under peak aging condition as shown in Fig. 5. A large amount of dislocation and small precipitation could be found along those dislocation ledges in Fig. 5(a) and

Fig. 5(b). The observed image in Fig. 5(c), which is a bright-field TEM photograph, presents two types of the precipitates. Type 1 consists of short relatively thin precipitates randomly distributed in the matrix while type 2 consists of longer, and thicker precipitates along the dislocation. The SAED patterns in Fig. 5(e) confirm the existence of  $\theta'$  and S' phases where its spots are denoted by red and blue arrows, respectively. In region A of Fig. 5(d), precipitates shaped as lath of phase S' extend in the direction of perpendicular  $(1\overline{10})$ Al. Zooming in view of the white rectangle in Fig. 5(f), it could be the Cu layer in the S phase. Compared to sample H01, sample H02 reveals that the peakaging microstructure is quite different, with the as-formed lath-shaped precipitates being the most visible components in this condition.

Based on the obtained results, the effects and mechanisms of pre-aging at 35°C and pre-aging at 0°C on the precipitation behavior during artificial aging can be further elucidated with the diagram shown in Fig. 6. In the case of pre-aging at 0°C, during the subsequent artificial aging, the formation of clusters or Guinier-Preston (GP) zones is restricted, these regions act as nucleation sites for the  $\beta''$  phase [13]. Thus, the nucleation of the  $\beta''$  phase is promoted, and continued artificial aging leads to the formation of other critical phases such as S', C, and E. However, the effect of deformation after pre-aging at 0°C

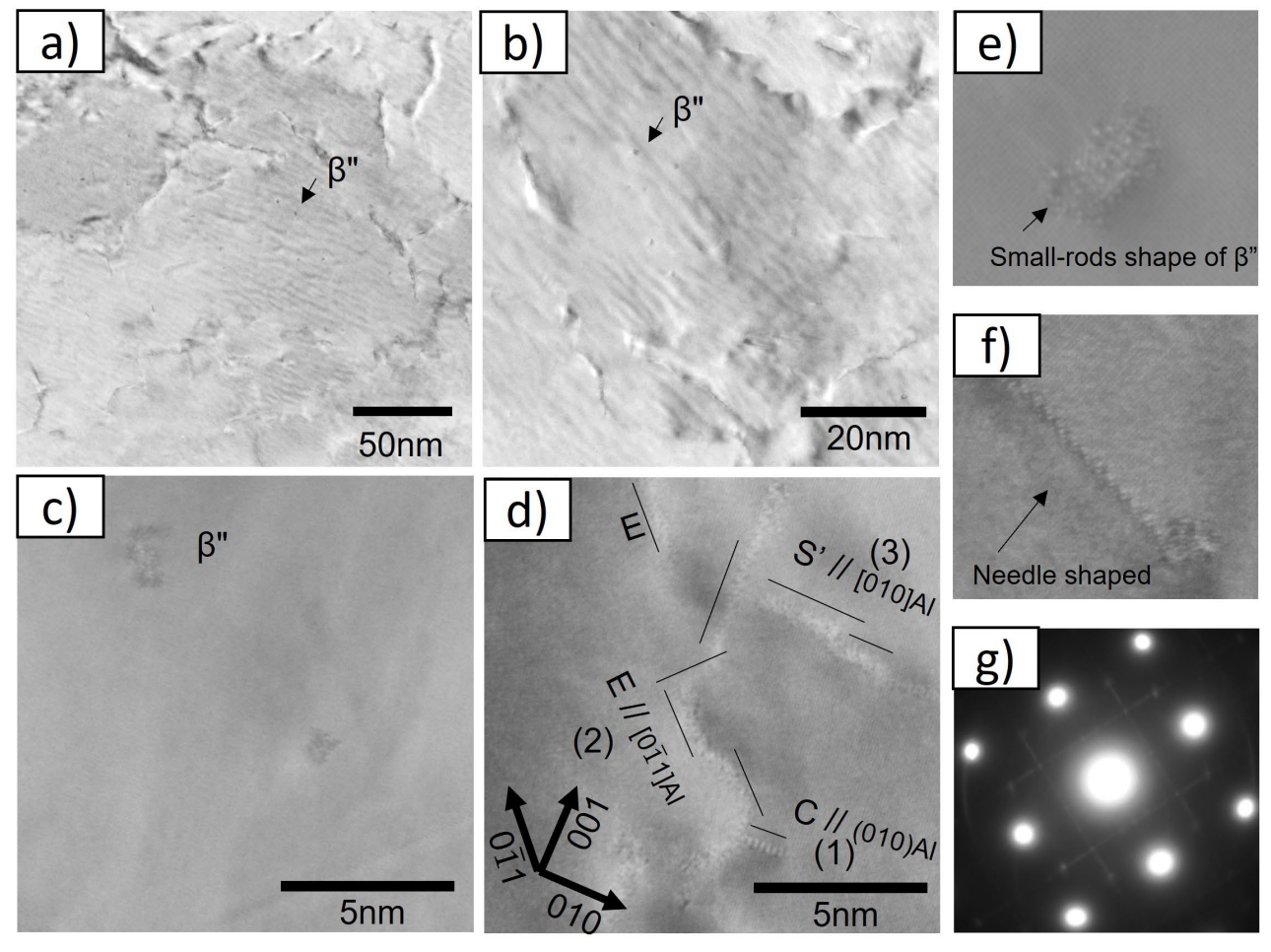


Fig. 4. (a-f) Bright-field TEM images of H01, pre-aging 0°C, deformation 30%, artificial aging 160°C at peak aging time; and (g) corresponding SEAD pattern

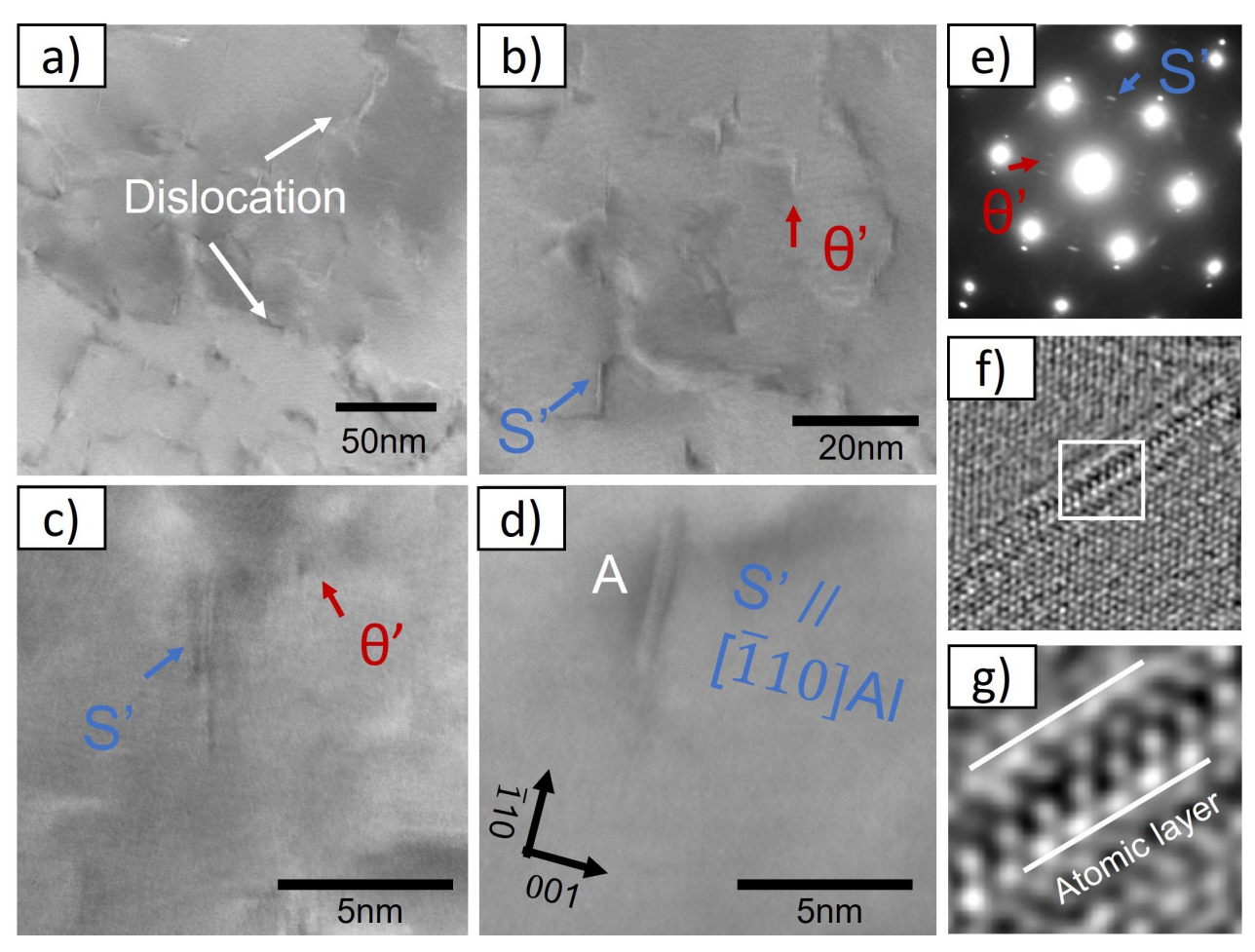


Fig. 5. (a, d) Bright-field TEM images of H02, pre-aging 35°C, deformation 30%, artificial aging 160°C at peak aging time; (e) corresponding SEAD pattern; (f) corresponding FFT from A area in Fig. 5(d); and (g) enlarged A area of white square in Fig. 5(f)

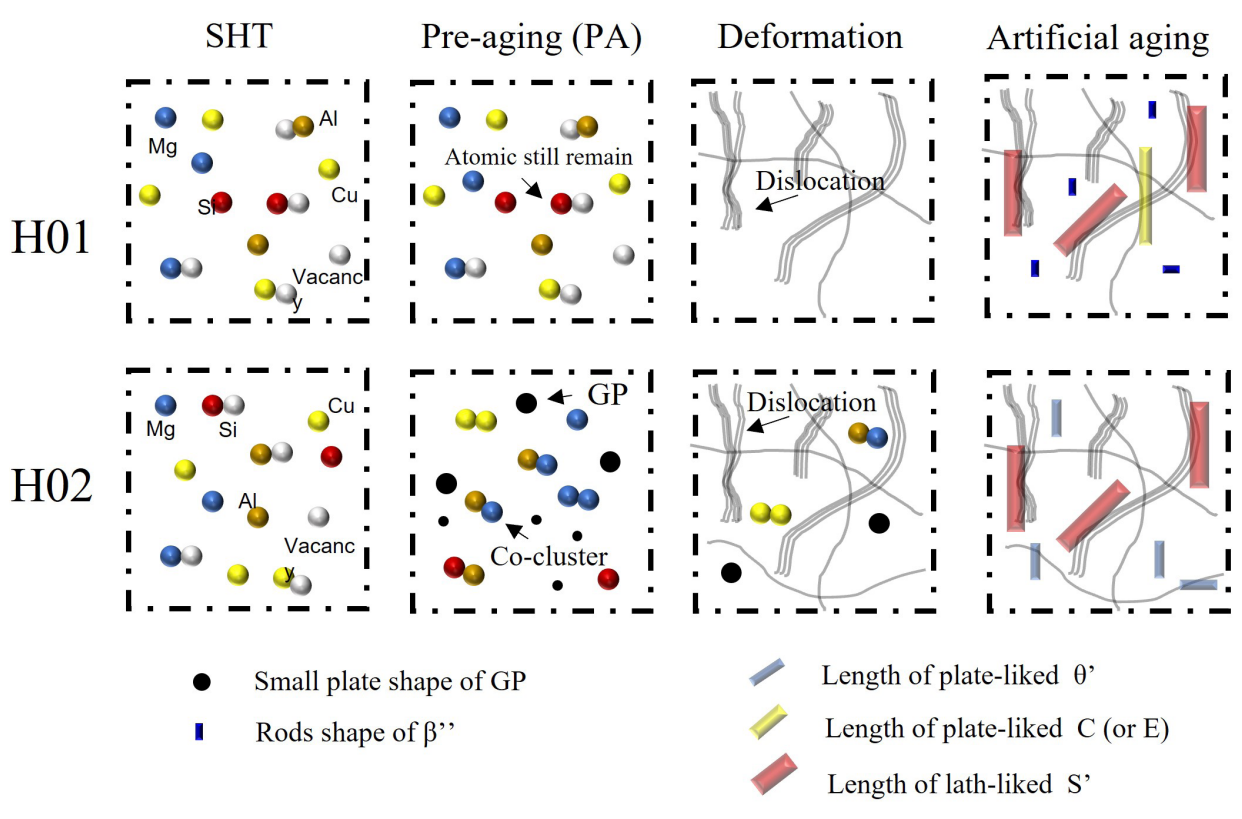


Fig. 6. Schematic diagram of the precipitation process of precipitated phase

on the strength and microstructure remains controversial. For example, Lai et al. [18] reported that pre-deformation-induced dislocations could enhance the age-hardening effect in some alloys while suppressing it in others. Therefore, the effect of pre-deformation on subsequent artificial aging depends on the alloy composition and the aging process, and the present study supports this conclusion.

Rometsch et al. [14] noted that natural aging after solution treatment without cold treatment leads to many solute clusters or Guinier-Preston (GP) zones. However, the concentration of dissolved atoms in the matrix is slightly reduced. Also, when deformation is applied after pre-aging at 35°C, the precipitation process may be interrupted by dislocations before further aging. In sample H02 deformed during peak aging, S' precipitates are promoted to form along dislocations, whereas  $\theta'$  precipitates may result from the transformation of cluster/GP zones. During the subsequent deformation process, these cluster/GP zones are gradually sheared by dislocation motion, which reduces the thermal stability of the sheared GP zones [15], and artificial aging at 160°C, some of these clusters/GP zones may become unstable and dissolve into the matrix, while others may develop into different phases [17]. The formation of precipitation and the growth of new precipitates also occur during artificial aging due to the high solute concentration in the matrix [5]. In addition to the precipitates forming along the dislocations, other phases may precipitate from the enriched zones [16].

#### 4. Conclusions

This study investigated the effect of pre-aging on the hardening behavior and precipitation response of Al-Cu-Mg-Si alloys during subsequent artificial aging. The main conclusions are as follows:

- Pre-aging improved the strength of all tested alloys, especially the medium strength alloys, regardless of the pre-aging temperature. Different pre-aging temperature result in similar strength improvements, but the hardness levels are different, with higher pre-aging temperature resulting in higher hardness.
- Pre-aging leads to increased dislocation density after deformation by promoting atomic diffusion. This diffusioninduced mechanism would help us to contribute to the dislocation density and understanding of structural properties.
- Pre-ageing temperature determines the precipitation patterns formed during the peak aging. The difference in this pre-aging temperature is a key factor that can affect the precipitation process.

#### Acknowledgments

We are deeply thankful to YKK Corporation for supplying the alloy used in this research. The results were presented during 14th Polish Japanese Joint Seminar on Micro and Nano Analysis (3-6.09.2024, Toyama, Japan).

#### REFERENCES

- W.J. Joost, Reducing vehicle weight and improving US energy efficiency using integrated computational materials engineering. Jom. 64, 1032-1038 (2015).
  - DOI: https://doi.org/10.1007/s118370120424z
- [2] L. He, H. Zhang, J. Cui, Effects of pre-ageing treatment on subsequent artificial ageing characteristics of an Al-1.01Mg-0.68Si-1.78Cu alloy. Journal of Materials Science & Technology 26 (2), 141-145 (2010).
  - DOI: https://doi.org/10.1016/S1005-0302(10)60023-0
- [3] M. Torsæter, H.S. Hasting, W. Lefebvre, C.D. Marioara, J.C. Walmsley, S.J. Andersen, R. Holmestad, The influence of composition and natural aging on clustering during preaging in Al–Mg–Si alloys. Journal of Applied Physics 108 (7), (2010). DOI: https://doi.org/10.1063/1.3481090
- [4] L. Cao, A.R. Paul, J.C. Malcolm, Clustering behaviour in an Al-Mg-Si-Cu alloy during natural ageing and subsequent underageing. Materials Science and Engineering A. 559, 257-261 (2013). DOI: https://doi.org/10.1016/j.msea.2012.08.093
- [5] Y. Zou, W. Xiaodong, T. Songbai, W. Yichang, Z. Kai, L. Cao, The effect of pre-ageing/stretching on the ageing-hardening behavior of Al–Zn–Mg–Cu alloys correlated with Zn/Mg ratio. Materials Science and Engineering A 830, 142331 (2020). DOI: https://doi.org/10.1016/j.msea.2021.142331
- [6] G.J. Gao, Y. Li, Z.D. Wang, R.D.K. Misra, H.S. Di, J.D. Li, G.M. Xu, Interaction between natural aging and pre-aging processes and its impact on the age-hardening behavior of Al-Mg-Si automotive sheets. JOM 71, 4405-4413 (2019). DOI: https://doi.org/10.1007/s11837019037806
- [7] Z. Li, Z. Roujin, Z. Pizhi, J. Zhihong, Effects of pre-aging and natural aging on the clusters, strength and hemming performance of AA6014 alloys. Materials Science and Engineering A 782, 139206 (2020). DOI: https://doi.org/10.1016/j.msea.2020.139206
- [8] V. Fallah, K. Andreas, O.O. Nana, G.M.R. Babak, P. Nikolas, E. Shahrzad, Atomic-scale pathway of early-stage precipitation in Al–Mg–Si alloys. Acta Materialia 82, 457-467 (2015). DOI: https://doi.org/10.1016/j.actamat.2014.09.004
- J.H. Kim, I. Jiwoo, S. Minyoung, K. Insu, Effects of Mg addition and pre-aging on the age-hardening behavior in Al-Mg-Si. Metals 8 (12), 1046 (2018).
   DOI: https://doi.org/10.3390/met8121046
- [10] C.D. Marioara, J. Andersen, T.N. Stene, H. Hasting, J. Walmsley, A.T.J. Van Helvoort, R. Holmestad, The effect of Cu on precipitation in Al–Mg–Si alloys. Philosophical Magazine 87 (23), 3385-3413 (2007). DOI: https://doi.org/10.1080/14786430701287377
- [11] E. Thronsen, C.D. Marioara, J.K. Sunde, K. Minakuchi, T. Katsumi, I. Erga, S.J. Andersen, The effect of heavy deformation on the precipitation in an Al-1.3 Cu-1.0 Mg-0.4 Si wt.% alloy. Materials & Design 186, 108203 (2020).
  - DOI: https://doi.org/10.1016/j.matdes.2019.108203
- [12] L. Korarik, M.J. Mills, Ab initio analysis of Guinier–Preston–Bagaryatsky zone nucleation in Al–Cu–Mg alloys. Acta Materialia 60 (9), 3861-3872 (2012).
  DOI: https://doi.org/10.1016/j.actamat.2012.03.044

- [13] D. Yin, Q. Xiao, Y. Chen, H. Liu, D. Yi, B. Wang, S. Pan, Effect of natural ageing and pre-straining on the hardening behaviour and microstructural response during artificial ageing of an Al-Mg-Si-Cu alloy. Materials & Design 95, 329-339 (1016). DOI: https://doi.org/10.1016/j.matdes.2016.01.119
- [14] P.A. Rometsch, Z. Xu, H. Zhong, H. Yang, L. Ju, X.H. Wu, Strength and Electrical Conductivity Relationships in Al-Mg-Si and Al-Sc Alloys. In Materials Science Forum (794-796, 827-832). Trans Tech Publications, Ltd.
  - DOI: https://doi.org/10.4028/www.scientific.net/msf.794-796.827
- [15] S.N. Khangholi, M. Javidani, A. Maltais, X.G. Chen, Effects of natural aging and pre-aging on the strength and electrical conductivity in Al-Mg-Si AA6201 conductor alloys. Materials Science and Engineering A 820, 141538 (2021). DOI: https://doi.org/10.1016/j.msea.2021.141538
- [16] H. Li, M. Qingzhong, Z. Wang, F. Miao, B. Fang, R. Song, Z. Zheng, Simultaneously enhancing the tensile properties and intergranular corrosion resistance of Al-Mg-Si-Cu alloys by a thermo-mechanical treatment. Materials Science and Engineering A 617, 165-174 (2014).
  - DOI: https://doi.org/10.1016/j.msea.2014.08.045
- [17] A. Deschamps, Y.J.A.M. Brechet, Influence of predeformation and ageing of an Al–Zn–Mg alloy – II. Modeling of precipitation kinetics and yield stress. Acta Materialia 47 (1), 293-305 (1998). DOI: https://doi.org/10.1016/S1359-6454(98)00296-1
- [18] Y.X. Lai, W. Fan, M.J. Yin, C.L. Wu, J.H. Chen, Structures and formation mechanisms of dislocation-induced precipitates in relation to the age-hardening responses of Al-Mg-Si alloys. Journal of Materials Science & Technology 41, 127-138 (2020). DOI: https://doi.org/10.1016/j.jmst.2019.11.001

- [19] G.K. Williamson, W.H. Hall, X-ray line broadening from filed aluminium and wolfram. Acta Metallurgica 1 (1), 22-31 (1953). DOI: https://doi.org/10.1016/0001-6160(53)90006-6
- [20] R. Kužel, Kinematical diffraction by distorted crystals—dislocation X-ray line broadening. Zeitschrift für Kristallographie-Crystalline Materials 222 (4), 136-149 (2007).
  DOI: https://doi.org/10.1524/zkri.2007.222.3-4.136
- [21] S. Takebayashi, T. Hunieda, N. Yoshinaga, K. Ushioda, S. Ogata, Comparison of the dislocation density in martensitic steels evaluated by some X-ray diffraction methods. ISIJ international 50 (6), 875-882 (2010).
  - DOI: https://doi.org/10.2355/isijinternational.50.875
- [22] T. Ungár, A. Borbély, The effect of dislocation contrast on x-ray line broadening: A new approach to line profile analysis. Applied Physics Letters 69 (21), 3173-3175 (1996). DOI: https://doi.org/10.1063/1.117951
- [23] T. Ungár, Dislocation densities, arrangements and character from X-ray diffraction experiments. Materials Science and Engineering A 309, 14-22 (2001). DOI: https://doi.org/10.1016/S0921-5093(00)01685-3
- [24] G. Ribárik, T. Ungár, Characterization of the microstructure in random and textured polycrystals and single crystals by diffraction line profile analysis. Materials Science and Engineering A 528 (1), 112-121 (2010). DOI: https://doi.org/10.1016/j.msea.2010.08.059
- [25] C. Y. Wang, C. M. Cededa-Jimenez, M. T. Pérez-Prado, Dislocation-particle interactions in magnesium alloys. Acta Materialia **194**, 190-206 (2020).
  - DOI: https://doi.org/10.1016/j.actamat.2020.04.055